Superhydrophobic Surfaces Having Two-Fold Adjustable Roughness Prepared in a Single Step

Laura Vogelaar, Rob G. H. Lammertink,* and Matthias Wessling

Membrane Technology Group, Faculty of Science and Technology, University of Twente, P.O. Box 217, Enschede, NL 7500 AE, The Netherlands

Received October 5, 2005. In Final Form: January 25, 2006

A fast and reliable method is reported for fabricating superhydrophobic surfaces. The method combines microstructure replication with polymer phase inversion and can be applied to a wide variety of polymers. This method provides a surface that contains roughness on two independently controllable levels, i.e., the microstructure level and the level of porosity stemming from the phase inversion. Both levels were optimized separately, resulting in water contact angles up to 167°.

1. Introduction

Nature has established a highly effective way to deal with contaminating particles. The leaves of certain plants and many insects exhibit superhydrophobicity.[1−5] Water does not show any affinity for the surface, causing water drops to behave very extraordinarily, e.g., bouncing and rolling instead of sliding.[6−8] When water droplets roll of such surfaces, they drag along dirt particles, which explains their self-cleaning character. A well-known example of a plant having a self-cleaning surface on its leaves is the lotus. Wax crystals on the lotus leaf create a very rough surface structure, which enhances the hydrophobicity. The sub-micrometer wax crystals form pillars with micrometer-scale dimensions. The texture on the leaves consequently consists of a 2-fold roughness, originating from the pillar structure and the wax crystals.[1,3] Therefore, outstanding self-cleaning properties for artificial surfaces can be expected if the 2-fold roughness structure of the lotus leaf is mimicked.[9−11] This paper describes how the combination of porosity and microstructure results in superhydrophobicity. Moreover, we show that both levels of roughness can be easily adjusted independently from each other, which distinguishes the fabrication method described here from alternative processes.

Synthetic surfaces that display a self-cleaning effect can find use in applications including microfluidics and macroscale antifouling layers. Surfaces with random-roughness structures have been fabricated out of a very wide diversity of materials. Among them are roughened poly(tetrafluroethylene) (PTFE) surfaces,[12−15] polypropylene after thermally induced phase separation,[16] fractal surfaces of alkylketene dimer,[17] several structures of carbon nanotubes,[18,19] some of which were coated with PTFE to enhance the hydrophobicity,[20] nanofibers of poly-(vinyl alcohol)[21] and polyacrylonitrile,[22] poly(methyl methacrylate) and fluorine-end-caped polyurethane blends,[23] poly-(acrylonitrile-*co*-α,α-dimethyl *meta*-isopropenylbenzyl isocyanate) with perfluorinated linear diol prepared by electrospinning,[24] polystyrene prepared by electrohydrodynamics,[25] phase-separated tetraethyl orthosilicate coated with fluoroalkylsilane,[26] and aluminum structured in various ways.[27]

Another approach to increase the surface area and thus the roughness is microstructuring surfaces. These surfaces have the additional advantage that they are attractive model surfaces, where the regularity of the pattern and the shape of the microstructures is very well defined and controlled. Microfabricated ultrahydrophobic surfaces have been made out of silicon, which was subsequently coated with a hydrophobic material (e.g., a silane),[28−30] SU-8 photoresist treated with a hydrophobic coating,[31] or poly(dimethylsiloxane) by means of replica molding.[32,33] Very recently, poly(dimethylsiloxane) replicas of natural

* To whom correspondence should be addressed. E-mail: R.G.H.Lammertink@utwente.nl.

(1) Neinhuis, C.; Barthlott, W. *Ann. Bot.-London* **1997,** *79,* 667.
(2) Blossey, R. *Nat. Mater.* **2003,** *2,* 301.
(3) Otten, A.; Herminghaus, S. *Langmuir* **2004,** *20,* 2405.
(4) Watson, G. S.; Watson, J. A. *Appl. Surf. Sci.* **2004,** *235,* 139.
(5) Barthlott, W.; Neinhuis, C. *Planta* **1997,** *202,* 1.
(6) Quéré, D. *Physica A* **2002,** *313,* 32.
(7) Richard, D.; Quéré, D. *Europhys. Lett.* **2000,** *50,* 769.
(8) Richard, D.; Quéré, D. *Europhys. Lett.* **1999,** *48,* 286.
(9) Patankar, N. A. *Langmuir* **2004,** *20,* 8209.
(10) Acatay, K.; Simsek, E.; Ow-Yang, C.; Menceloglu, Y. Z. *Angew. Chem., Int. Ed.* **2004,** *43,* 5210.
(11) Sun, M.; Luo, C.; Xu, L.; Ji, H.; Ouyang, Q.; Yu, D.; Chen, Y. *Langmuir* **2005,** *21,* 8978.
(12) Minko, S.; Mueller, M.; Motornov, M.; Nitschke, M.; Grundke, K.; Stamm, M. *J. Am. Chem. Soc.* **2003,** *125,* 3896.
(13) Veeramasuneni, S.; Drelich, J.; Miller, J. D.; Yamauchi, G. *Prog. Org. Coat.* **1997,** *31,* 265.

(14) Chen, W.; Fadeev, A. Y.; Hsieh, M. C.; Oner, D.; Youngblood, J.; McCarthy, T. J. *Langmuir* **1999,** *15,* 3395.
(15) Zhang, J.; Li, J.; Han, Y. *Macromol. Rapid Comm.* **2004,** *25,* 1105.
(16) Erbil, H. Y.; Demirel, A. L.; Avci, Y.; Mert, O. *Science* **2003,** *299,* 1377.
(17) Shibuichi, S.; Onda, T.; Satoh, N.; Tsujii, K. *J. Phys. Chem.* **1996,** *100,* 19512. Onda, T.; Shibuichi, S.; Satoh, N.; Tsujii, K. *Langmuir* **1996,** *12,* 2125.
(18) Li, S.; Li, H.; Wang, X.; Song, Y.; Liu, Y.; Jiang, L.; Zhu, D. *J. Phys. Chem. B* **2002,** *106,* 9274.
(19) Li, H.; Wang, X.; Song, Y.; Liu, Y.; Li, Q.; Jiang, L.; Zhu, D. *Angew. Chem., Int. Ed.* **2001,** *40,* 1743.
(20) Lau, K. K. S.; Bico, J.; Teo, K. B. K.; Chhowalla, M.; Amaratunga, G. A. J.; Milne, W. I.; McKinley, G. H.; Gleason, K. K. *Nano Lett.* **2003,** *3,* 1701.
(21) Feng, L.; Song, Y.; Zhai, J.; Liu, B.; Xu, J.; Jiang, L.; Zhu, D. *Angew. Chem.* **2003,** *115,* 824.
(22) Feng, L.; Li, S.; Li, Y.; Li, H.; Zhang, L.; Zhai, J.; Song, Y.; Liu, B.; Jiang, L.; Zhu, D. *Adv. Mater.* **2002,** *14,* 1857.
(23) Xie, Q.; Xu, J.; Feng, L.; Jiang, L.; Tang, W.; Luo, X.; Han, C. C. *Adv. Mater.* **2004,** *16,* 302.
(24) Acatay, K.; Simsek, E.; Ow-Yang, C.; Menceloglu, Y. Z. *Angew. Chem. Int. Ed.* **2004,** *43,* 5210.
(25) Jiang, L.; Zhao, Y.; Zhai, J. *Angew. Chem., Int. Ed.* **2004,** *43,* 4338.
(26) Nakajima, A.; Abe, K.; Hashimoto, K.; Watanabe, T. *Thin Solid Films* **2000,** *376,* 140.
(27) Thieme, M.; Frenzel, R.; Schmidt, S.; Simon, F.; Hennig, A.; Worch, H.; Lunkwitz, K.; Scharnweber, D. *Adv. Eng. Mater.* **2001,** *3,* 691.
(28) Oner, D.; McCarthy, T. J. *Langmuir* **2000,** *16,* 7777.
(29) Yoshimitsu, Z.; Nakajima, A.; Watanabe, T.; Hashimoto, K. *Langmuir* **2002,** *18,* 5818.
(30) Bico, J.; Marzolin, C.; Quere, D. *Europhys. Lett.* **1999,** *47,* 220.
(31) Shirtcliff, N. J.; Aqil, S.; Evans, C.; McHale, G.; Newton, M. I.; Perry, C. C.; Roach, P. *J. Micromech. Microeng.* **2004,** *14,* 1384.
(32) He, B.; Patankar, N. A.; Lee, J. *Langmuir* **2003,** *19,* 4999.
(33) Jopp, J.; Gruell, H.; Yerushalmi-Rozen, R. *Langmuir* **2004,** *20,* 10015.

lotus leaves also were reported to display superhydrophobicity.[34] The surface texture with hierarchal structure on two length scales is responsible for the enhanced hydrophobicity.

Ultimately, for a superhydrophobic surface in a commercial application, simplicity and cost-effectiveness of the fabrication process and accessibility of the materials are desired. Besides, for most uses, the mechanical stability of the surface is important.[26] Many of the current preparation routes are not very straight-forward, e.g., they require vacuum equipment, require many fabrication steps, or are time-consuming.

Here we present a fabrication process which combines microfabrication with a random roughness. In this way, a hierarchical roughness structure is created, of which both roughness levels can be controlled independently. The method, named phase-separation micro molding (PSμM), is applicable on virtually any soluble polymer, which opens up a very wide range of materials and, consequently, surface properties.[35,36] The fabrication process can be used to truly mimic the 2-fold roughness structure of the lotus leaf in a single-step process and provides a very simple preparation route to superhydrophobicity in a synthetic surface.

There are a few other preparation processes that yield superhydrophobic surfaces with roughness on multiple length scales.[18,22,23,25] In structures of aligned carbon nanotubes, the nanotubes form the superimposed roughness.[18,22] Another example is the incorporation of porous microspheres.[25] Surfaces prepared by drying of solutions of poly(methyl methacrylate) and fluorine-end-capped polyurethane blends arrange the polymer in microstructures, having an additional roughness on the nanometer level.[23] The enhancement of the self-cleaning proper-ties that is predicted by theory is indeed confirmed experimentally for these surfaces.[9,37] The advantage of PSμM is that both levels of the roughness are controlled by different process parameters and can therefore be tailored individually to optimize the hydrophobicity.

On a self-cleaning surface, generally a water drop bridges the gap between the protrusions of the rough material. Such 'fakir' droplets exhibit a contact angle according to the Cassie–Baxter equation:[38] $\cos \theta_{CB} = -1 + \Phi_s(1 + \cos \theta)$, in which θ is the contact angle on a flat, smooth surface, θ_{CB} is the predicted angle on the rough surface, and Φ_s is the surface solid fraction; the ratio between the water contacted and the total projected surface area. This expression of the Cassie–Baxter equation describes only the ideally nonwetting case. The equation does not take into account that the drop might actually wet an area that is slightly larger than the surface solid fraction because the liquid may partly penetrate into the grooves.[39] Additionally, on self-cleaning surfaces, there is very little hysteresis between advancing and receding contact angle, predicting a low sliding angle: a very small inclination may cause the drop to roll off instantaneously.

2. Experimental Section

Preparation of the Surfaces. Hyflon AD 80X and Hyflon AD 60X were obtained from Solvay Solexis. Both materials were dissolved in HGalden ZT 130, which was also acquired from Solvay Solexis. The polymers were dissolved in different concentrations between 10 and 20 wt% at ambient room temperature under constant stirring.

The mold was prepared from silicon by photolithography and etching. The etching was performed on a Plasmatherm SLR 770, using a standard Bosch process (C_4F_8, SF_6, and Ar gas). The silicon substrate was maintained at a temperature of 20 °C. One cycle consisted of 2 s of deposition, 2 s of removal, and 6 s of etching. The final depth of the mold was 8 μm. The height of the microstructures from the optimized recipe (see below) is measured to match the 8-μm depth of the mold.

The solutions were spread out by casting a film that has a thickness of 100 μm for PSμM and 250 μm for evaporation. Immersion precipitation was performed in *n*-pentane (98%, Acros). The polymer was kept on the mold in pentane for approximately half an hour and was subsequently rinsed in ethanol (analytical quality, Merck) for another half hour. Evaporation of solvent succeeded in a nitrogen environment at ambient room temperature for ~20 h. To prevent the polymer films from curling, they were either dried while clamped between glass slides or were attached on thin glass slides coated with double-sided sticky tape. In the latter case, the coated side of the glass plate was applied on the backside of the structured polymer film, while the film was floating and spread on water. In this way, the polymer was completely flat on the glass plate. The films were dried in air.

Contact Angle Measurements. Contact angle measurements were performed on a Goniometer (Dataphysics OCA 15+). Initially, the surfaces resulting from different PSμM recipes were screened by measuring static contact angles, using drops having a volume of 6 μL. Advancing and receding contact angles were determined by placing the needle in the drop and continuously supplying or withdrawing water. The sliding angle was determined by placing the glass plate, on which the polymer was coated, on a leveled surface. The surface was inclined gradually, placing a drop of 11 μL on the surface after each inclination step.

Electron Microscopy. The SEM observations were performed on a JEOL 5600 LV electron microscope. An acceleration voltage of 5 kV was applied. Prior to imaging, the polymeric samples were coated with a thin layer of platinum (~25 nm thick) to avoid charging of the samples.

Atomic Force Microscopy. The AFM measurements were performed on a Nanoscope III (Digital Instruments) operating in tapping mode.
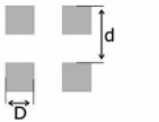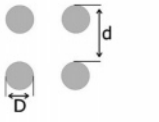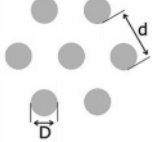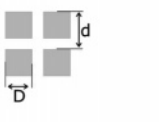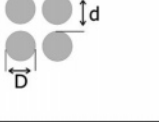
3. Results and Discussion

In PSμM, a polymer solution is applied on a mold, which has a micrometer-sized relief profile on its surface. Subsequently, mold and solution are immersed in a nonsolvent. The nonsolvent and solvent exchange, causing the polymer to solidify and assimilate the structure on the mold. PSμM is a very reliable, simple, and cost-effective replication method.[35,35] The fabrication of the surface requires only a single, simple, and fast fabrication step. The minimum feature size that can be achieved for PSμM is typically 1 μm. However, depending on the recipe, feature sizes down to 150 nm can be achieved. Aspect ratios of the structures can be as high as 5.

The porosity stems directly from the use of liquid-induced phase separation in the process. The polymer solution separates in a polymer-lean and a polymer-rich part. The polymer-rich part will form the solid polymer, while the polymer-lean part can cluster in the polymer and form pores.[40,41] By adjusting the composition of the solvent and nonsolvent, the phase-separation process can yield highly porous, as well as dense, materials. Accordingly, the porosity in a microstructure prepared by PSμM can be tailored by tuning the recipe.[35] The use of microfabrication has the advantage that the design of the microstructure can be chosen in any size or shape. Therefore, both roughness levels

(34) Sun, M.; Luo, C.; Xu, L.; Ji, H.; Ouyang, Q.; Yu, D.; Chen, Y. *Langmuir* **2005**, *21*, 8978.

(35) Vogelaar, L.; Barsema, J. N.; van Rijn, C. J. M.; Nijdam, W.; Wessling, M. *Adv. Mater.* **2003**, *15*, 1385.

(36) Vogelaar, L.; Lammertink, R. G. H.; Barsema, J. N.; Nijdam, W.; Bolhuis-Versteeg, L. A. M.; van Rijn, C. J. M.; Wessling, M. *Small* **2005**, *1*, 645.

(37) Herminghaus, S. *Europhys. Lett.* **2000**, *52*, 165.

(38) Queré, D. *Nat. Mater.* **2002**, *1*, 14.

(39) Marmur, A. *Langmuir* **2004**, *20*, 3517.

(40) Mulder, M. *Basic Principles of Membrane Technology*; Kluwer Academic Publishers: Dordrecht, The Netherlands, 1996.

(41) Baker, R. W. *Membrane Technology and Research*; McGraw-Hill: New York, 2000.

Table 1. Measurements and predictions of contact angles on Hyflon AD 80X surfaces[a]

Pattern	Predicted contact angle (Cassie-Baxter)	Advancing and receding contact angle Evaporation	Advancing and receding contact angle PSµM
1. d= 10 µm Φ_s=0.25	θ_{CB}= 147	θ_a= 140 θ_r= 135	θ_a= 160 θ_r= 159
2. d= 10 µm Φ_s=0.20	θ_{CB}= 151	θ_a= 146 θ_r= 142	θ_a= 162 θ_r= 150
3. d= 10 µm Φ_s=0.23	θ_{CB}= 148	θ_a= 156 θ_r= 153	θ_a= 167 θ_r= 165
4. d= 7.07 µm Φ_s=0.50	θ_{CB}= 132	θ_a= 152 θ_r= 145	θ_a= 149 θ_r= 142
5. d= 10 µm Φ_s=0.50	θ_{CB}= 132	θ_a= 148 θ_r= 143	θ_a= 154 θ_r= 139
6. d= 6.27 µm Φ_s=0.50	θ_{CB}= 132	θ_a= 157 θ_r= 151	θ_a= 156 θ_r= 152

[a] The surfaces were either prepared by evaporation or by PSµM. The patterns on the microstructures consist of either pillars or square posts in different compositions, with $D = 5$ µm. The experimental error in the measurements is ~3°.

of the fabricated surface can be adjusted independently: the microstructure by control over the mold design and the porosity by control over the phase-separation recipe. This aspect distinguishes PSµM from the other methods that can achieve a hierarchal roughness, in which the roughness has a more complex correlation to the different process parameters.

Generally, hydrophobic flat surfaces can exhibit contact angles up to 120°.[2] The hydrophobic polymer Hyflon AD was chosen as a hydrophobic material that is suitable for processing by PSµM. For this material, which is a copolymer of tetrafluorethylene (TFE) and 2,2,4-trifluoromethoxy-1,3-dioxole (MDO), water contact angles up to 120° have been reported.[42,43] Moreover, the polymer is well soluble in perfluorinated solvents and is, therefore, easily applicable in PSµM. Two types of the polymer were processed, namely Hyflon AD 60X (composed of 60 mol% MDO
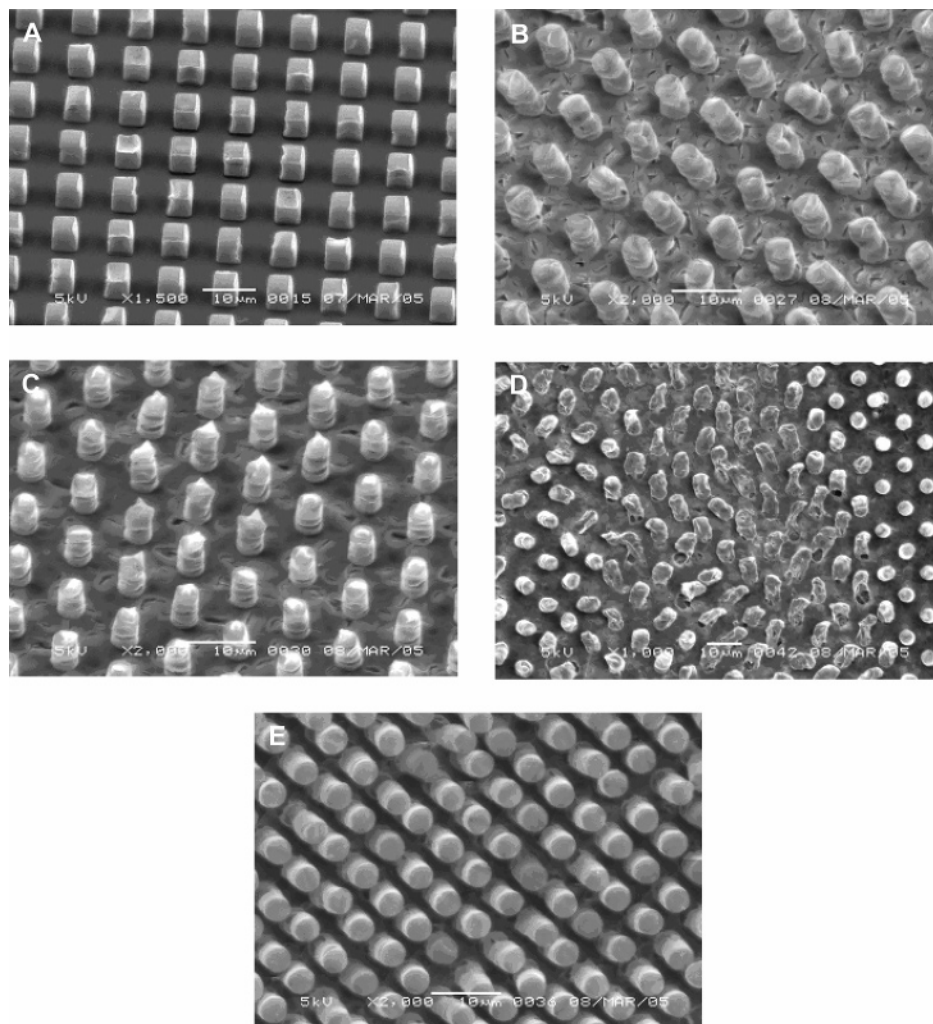
and 40 mol% TFE) and Hyflon AD 80X (composed of 80 mol% MDO and 20 mol% TFE). For simplicity, the two types of Hyflon AD will be abbreviated by H60 and H80 correspondingly. Although Hyflon is chosen here as an example, we like to emphasize that many more hydrophobic polymers can be processed that may lead to superhydrophobic surfaces.

To study the influence of the microstructure, six different patterns are prepared, each consisting of microstructures with a minimum feature size of 5 µm. The minimum feature size is chosen to mimic the typical size of the microstructures on the leaf of the lotus. The replicas formed by PSµM consist of either cylindrical or rectangular pillars. The different patterns have surface solid fractions around 0.5 or 0.2 (see Table 1).

Polymer solutions are prepared in different concentrations to vary the intrinsic porosity of the resulting film. Smooth microstructures are prepared by evaporation as well (see Figure 1A) to evaluate the effect of the intrinsic porosity introduced by the phase separation on the hydrophobicity. The structures

(42) Arcella, V.; Colaianna, P.; Maccone, P.; Sanguineti, A.; Gordano, A.; Clarizia, G.; Drioli, E. *J. Membr. Sci.* **1999**, *163*, 203.
(43) Gordano, A.; Arcella, V.; Drioli, E. *Desalination* **2004**, *163*, 127.

Figure 1. Surfaces prepared from Hyflon AD. Figure 1A shows a H80 structure of square pillars prepared by evaporating a 15 wt% solution on a mold. Figure 1B and C shows H80 microstructures of pillars, prepared by PSμM, illustrating the roughness superimposed on the microstructure. Figure 1D displays a surface of H60, prepared by PSμM from a solution with similar polymer concentration as the structures shown in Figure 1B and C. Figure 1E displays the protrusions of a microstructure of closely packed pillars, prepared by PSμM, with limited superimposed roughness.
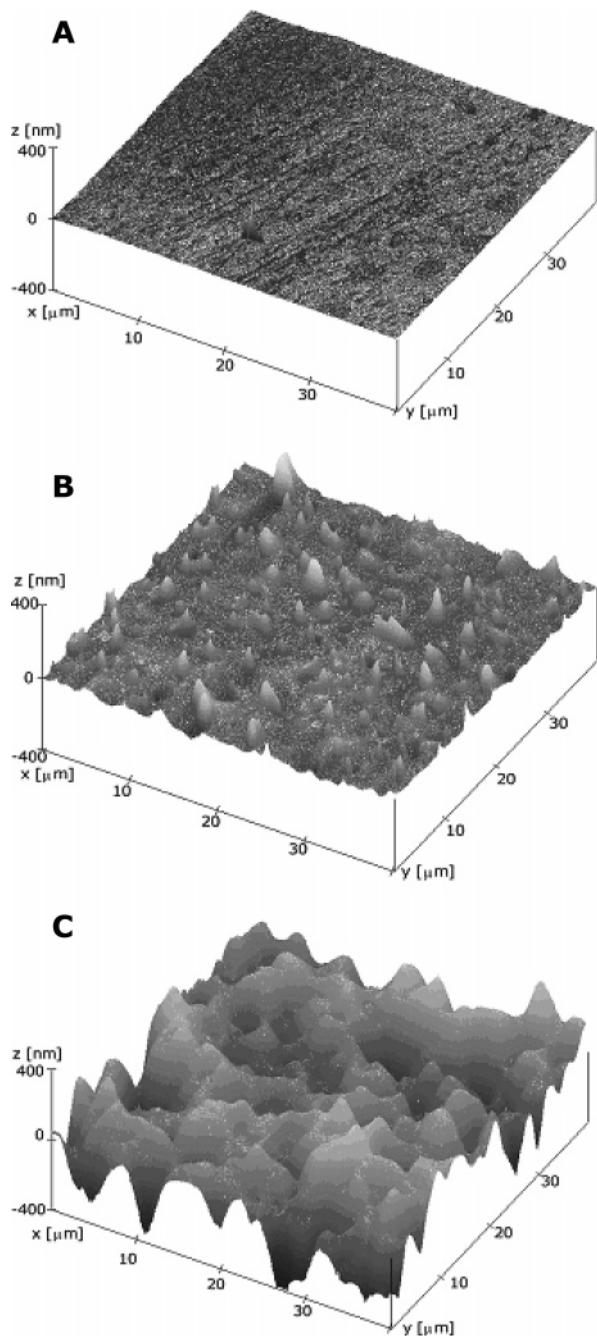
prepared by PSμM clearly display a superimposed roughness stemming from the combined micromolding and phase-separation process (Figure 1B and C). AFM measurements confirm that phase separation indeed increases the roughness (Figure 2). Sometimes the pillars of the microstructure even collectively demonstrate the formation of a sharp tip (Figure 1C). The presence of such a tip can further reduce the contact area of the droplet on the surface, lowering Φ_s, and therefore promote superhydrophobicity.

The different surfaces prepared by PSμM are initially screened by measuring the static contact angles. Subsequently, for the optimal phase-separation recipe, advancing and receding contact angles are determined. During the initial screening, it appeared that the contact angles measured on H80 surfaces prepared by PSμM are generally higher than the values on H60 surfaces. The better performance of H80 surfaces is somewhat surprising since a H60 surface prepared by phase separation is rougher than a similar H80 surface (see AFM images in Figure 2). Moreover, the contact angles on smooth H60 surfaces are slightly higher than those on H80, as expected from the higher fluor content. A possible explanation for the higher contact angle on structured H80 is found when the surfaces are observed by electron microscopy. A clear distinction in the robustness of the surfaces is evident (see Figure 1D). In some places, the microstructures

of H60 are damaged, whereas the structured H80 is unaffected by the handling for measurements. The inferior mechanical stability of H60 compared to H80 might be an explanation, although differences in pore morphology within the material may also have caused the higher sensitivity to deformations of H60. The presence of such deformations may explain the lower contact angles observed for water drops on H60 surfaces. Nevertheless, for H80 surfaces, the results are similar even after clamping them between two glass plates several times, and therefore, these surfaces appear to be robust.

Increasing the polymer concentration of the casting solution generally leads to a decrease of the porosity after phase separation and, therefore, decreases the roughness. If, on the other hand, the polymer concentration in the solution is too low, there is insufficient polymer to precisely assimilate the structure on the mold and form a stable microstructure. The optimal polymer solution, consequently, is the solution that contains just enough polymer to form a defect-free microstructure having maximum porosity (namely 17.5 wt%).

Table 1 resumes the advancing and receding contact angles for each pattern on H80 surfaces prepared by PSμM, in comparison to the values on a smooth, microstructured H80 surface prepared by evaporation. The expectations based on the Cassie−Baxter equation are calculated. The calculation only takes
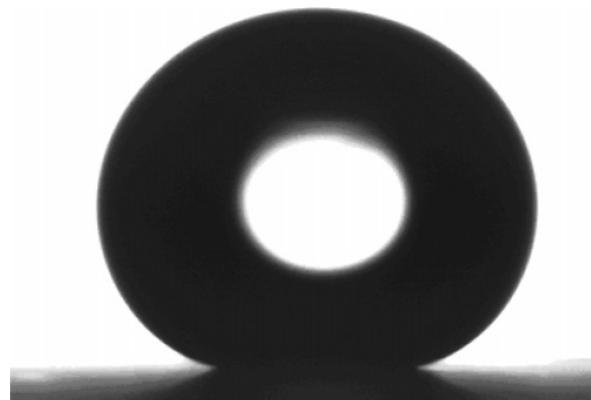
Figure 2. Atomic Force Microscopy on Hyflon AD surfaces. (A) H80 surface prepared by evaporation. (B) H80 surface prepared by phase separation of a 17.5 wt% solution. (C) H60 surface prepared by phase separation of a 17.5 wt% solution.

Figure 3. Water drop on a H80 surface patterned by PSμM, side view from a goniometer measurement. The water drop displays a contact angle above 160°.

lags behind the measurements. The deviation between calculation and measurement confirms that the presence of the microstructure influences the pore formation during phase inversion. Therefore, the microstructure enhances the surface roughness, as was observed already on the structure in Figure 1C.

The increase in contact angle for a phase-separated compared to an evaporated microstructure is much higher for the structures having a Φ_s around 0.2 (patterns 1−3) than for the structures having a Φ_s of 0.5 (patterns 4−6). In the latter case, sometimes there is even no detectable improvement in hydrophobicity stemming from the roughness caused by phase separation. The top part of the protrusions on patterns 4−6 appears to be hardly influenced by porosity (see Figure 1E). Although it is not yet clear why the roughness on these microstructures differs from similar microstructures in a less closely packed configuration (see Figure 1B and C), this phenomenon explains why there is little influence of the porosity on the measured contact angles for patterns 4−6.

Considering the contact angles measured on the different patterns, in most cases higher contact angles and less hysteresis are measured for the patterns with Φ_s around 0.2, compared to the patterns having a Φ_s of 0.5, as was predicted by the Cassie−Baxter equation. However, the Cassie−Baxter equation does not always give a correct prediction for the contact angles on smooth microstructures prepared by evaporation. Higher contact angles are measured especially for the three structures having a Φ_s of 0.5. Inaccuracy in the fabrication process of the mold cannot account for such high values. Deviations toward lower contact angles can be explained if the drop is not completely in the Cassie−Baxter regime and wets an area larger than merely the tops of the protrusions.[39]

Comparing different patterns with similar Φ_s, the hysteresis is clearly influenced by the possible contact lines that the water can form on the patterns, in agreement with theoretical predictions.[14] The shorter the contact lines between the surface and the water, the less the hysteresis, since the water is offered hardly any possibility to pin on the surface. In the data in Table 1, such pinning behavior is demonstrated by structure 5. The pattern is composed of the same pillar structure and additionally has the same Φ_s as the pattern in structure 4, but the pillars are arranged differently. The only explanation is that in structure 5 the contact line between the protrusions is longer, permitting pinning. The pillar pattern in a hexagonal lattice, structure 3, offers the least possibility for the drop to pin on the surface, and indeed the measurements indicate a very low hysteresis.

To confirm the superhydrophobic behavior, the sliding angle was determined on a surface patterned with structure 3. If the

the microstructure into account and is based on measurements of the contact angle on a smooth H80 surface ($\theta = 110°$). A typical example of a drop on a superhydrophobic Hyflon surface is depicted in Figure 3.

From the data in Table 1, it follows that the phase-separated microstructures generally provide higher contact angles and reduced hysteresis in comparison to microstructures prepared by evaporation. The improved superhydrophobicity demonstrates that the roughness originating from the phase separation mimics the function of the superimposed roughness of the lotus leaf.

Interestingly, the contact angles measured on the surfaces prepared by PSμM cannot be predicted by calculation. Using the contact angle measured on a flat H80 film prepared by phase inversion as input, the outcome of the Cassie−Baxter equation

surface was placed under a very small inclination angle of 0.5°, water drops can no longer stay on the surface and immediately roll off. The very low sliding angle confirms the superhydrophobic character of the surface.

4. Conclusions

In conclusion, PSμM is used to prepare superhydrophobic surfaces in a single process step. The superhydrophobicity stems from hierarchal roughness, consisting of a microstructure and a superimposed roughness caused by intrinsic porosity. This is concluded from measurements of water contact angles on microstructured surfaces prepared by PSμM, in comparison with results on smooth microstructured surfaces prepared by evaporation. In PSμM, both levels of roughness can be controlled independently: the microstructure by adjusting the patterns on the mold and the superimposed roughness by adaptation of the phase-separation recipe. Therefore, it is straightforward to tailor both levels of roughness to find the optimal hydrophobicity. For the surfaces that were optimized in terms of hydrophobicity, water contact angles as high as 167° have been obtained, showing hardly any contact angle hysteresis. If the surface is inclined by only 0.5°, drops can no longer rest on the surface and roll off. PSμM therefore proves to be a successful route for the preparation of superhydrophobic surfaces.